Inorganic Chemistry

ARTICLE

pubs.acs.org/IC

Synthesis, Structures, and Magnetism of Copper(II) and Manganese(II) Coordination Polymers with Azide and Pyridylbenzoates

Xiu-Mei Zhang,[†,‡] Yan-Qin Wang,[†] You Song,[§] and En-Qing Gao*[,†]

[†]Shanghai Key Laboratory of Green Chemistry and Chemical Processes, Department of Chemistry, East China Normal University, Shanghai 200062, China

[‡]School of Chemistry and Materials Science, Huaibei Normal University, Huaibei, Anhui 235000, China

[§]State Key Laboratory of Coordination Chemistry, School of Chemistry and Chemical Engineering, Nanjing University, Nanjing 210093, China

Supporting Information

ABSTRACT: Three transition-metal coordination polymers with azide and/or carboxylate bridges have been synthesized from 4-(3-pyridyl)benzoic acid (4,3-Hpybz) and 4-(4-pyridyl)benzoic acid (4,4-Hpybz) and characterized by X-ray crystallography and magnetic measurements. Compound **1**, $[Cu(4,3\text{-pybz})(N_3)]_n$, consists of 2D coordination networks in which the uniform chains with (μ-EE-N_3)(μ-COO) double bridges are cross-linked by the 4,3-pybz ligands. Compound **2**, $[Cu_2(4,4\text{-pybz})_3(N_3)]_n \cdot 3nH_2O$, consists of 2-fold interpenetrated 3D coordination networks with the α-Po topology, in which the six-connected dinuclear motifs with mixed (μ-EO-N_3)(μ-COO)$_2$ (EO = end-on) triple bridges are linked by the 4,4-pybz spacers. Compound **3**, $[Mn(4,4\text{-pybz})(N_3)(H_2O)_2]_n$, contains 2D manganese(II) coordination networks in which the chains with single μ-EE-N_3 bridges (EE = end-to-end) are interlinked by the 4,4-pybz ligands, and the structure also features a 2D hydrogen-bonded network in which Mn^{II} ions are linked by double triatomic bridges, (μ-EE-N_3)(O−H···N) and (O−H···O)$_2$. Magnetic studies indicated that the mixed azide and carboxylate bridges in **1** and **2** induce ferromagnetic coupling between Cu^{II} ions and that **3** features antiferromagnetic coupling through the EE-azide bridge. In addition, compound **1** exhibits antiferromagnetic ordering below 6.2 K and behaves as a field-induced metamagnet. A magnetostructural survey indicates a general trend that the ferromagnetic coupling through the mixed bridges decreases as the Cu−N−Cu angle increases.

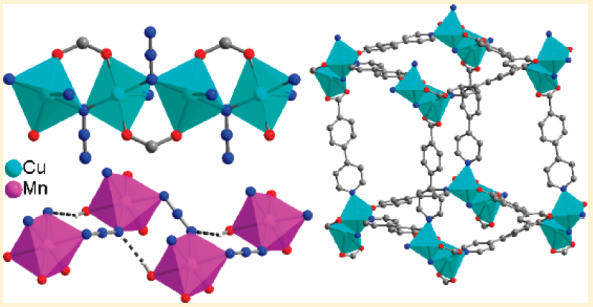

INTRODUCTION

The research of molecular magnetic systems has been of considerable interest for decades, aimed at elucidating fundamental magnetic phenomena, unveiling magnetostructural correlations, and constructing new magnetic materials with potential applications.[1,2] Coordination chemistry has been the most powerful tool to access such systems, and the general approach is to use short bridging groups to connect paramagnetic metal centers and to transmit magnetic coupling. Among the most frequently used bridging groups in this context, carboxylate and azide have exceptionally rich coordination chemistry and magnetochemistry, capable of linking metal ions in various modes and transmitting magnetic exchange of different nature and magnitude.[3] The rich chemistry challenges the designed assembly,[4] which is always pursued as an appealing approach to targeted and tunable structures or properties, but has offered great opportunities for serendipitous assembly, which is always an important approach to new structures or new properties.[5] To evoke the rich chemistry or sometimes to gain some control, various auxiliary organic ligands for azide and various backbones for carboxylate ligands have been introduced, leading to a large number of polynuclear aggregates or coordination polymers with diverse topologies and magnetic properties.[3,6−13]

Using azide and carboxylate as cobridges is an interesting approach to magnetic systems, but the cobridging of the two anionic groups may be impeded by the competition in coordination and charge balance. A limited number of cobridging systems have been synthesized from mono/dicarboxylate ligands [$RCOO^-$/$R(COO^-)_2$] (R = H, methyl, ethyl, and phenylene).[14−16] Recently, we have demonstrated that the zwitterionic mono/dicarboxylate ligands bearing self-compensated positive (pyridinium) and negative (carboxylate) charges can readily collaborate with azide to generate 1D, or sometimes 0D, 2D, or even 3D, magnetic motifs with simultaneous azide and carboxylate bridges, with interesting magnetic properties such as ferromagnetic coupling, solvent-modulated metamagnetism, and single-chain magnetism.[17,18] The pyridylcarboxylate bifunctional ligands such as pyridylcarboxylates and pyridylacrylates have also led to some cobridging systems, with various structures and magnetic properties.[19,20] As

Received: April 27, 2011
Published: July 06, 2011

an extension of the study, we report in this paper three coordination polymers derived from 4-(3-pyridyl)benzoate (4,3-pybz) and 4-(4-pyridyl)benzoate (4,4-pybz), $[Cu(4,3\text{-pybz})(N_3)]_n$ (**1**), $[Cu_2(4,4\text{-pybz})_3(N_3)]_n\cdot 3nH_2O$ (**2**), and $[Mn(4,4\text{-pybz})(N_3)(H_2O)_2]_n$ (**3**). All of these structures are different from those with pyridylcarboxylates. In **1**, the copper(II) chains with (μ-EO-N_3)(μ-COO) double bridges (EO = end-on) are connected into 2D layers by the 4,3-pybz spacers. In **2**, the novel dicopper motifs with (μ-EO-N_3)(μ-COO)$_2$ triple bridges are linked by 4,4-pybz to generate 3D frameworks with 2-fold interpenetration. Compound **3** consists of 2D coordination networks in which the manganese(II) chains with single μ-EE-N_3 bridges (EE = end-to-end) are linked by 4,4-pybz ligands, and the structure is reinforced by the O−H···N and O−H···O triatomic bridges between Mn^{II} ions. Magnetic studies indicated that the mixed bridges in **1** and **2** induce ferromagnetic coupling between Cu^{II} ions and that **3** features antiferromagnetic coupling along the EE-azide-bridged chain. In addition, **1** behaves as a metamagnet. A magnetostructural survey indicates a general trend that the ferromagnetic coupling through the mixed bridges decreases as the Cu−N−Cu angle increases.

EXPERIMENTAL SECTION

Materials and Physical Measurements. All of the solvents and reagents including 4,3-Hpybz and 4,4-Hpybz were purchased commercially (Sinopharm and Alfa Aesar) and were used as received. IR spectra were recorded on a Nexus 670 FT-IR spectrometer using KBr pellets. Elemental analysis was carried out on an Elementar Vario El III elemental analyzer. Temperature- and field-dependent magnetic measurements were carried out on a Quantum Design SQUID MPMS-5 magnetometer. Diamagnetic corrections were made with Pascal's constants.

Caution! *Although not encountered in our experiments, azide compounds of metal ions are potentially explosive. Only a small amount of the materials should be prepared, and it should be handled with care.*

$[Cu(4,3\text{-pybz})(N_3)]_n$ (1). In a test tube, a solution of 4,3-Hpybz (0.010 g, 0.05 mmol) and NaN_3 (0.013 g, 0.2 mmol) in water (3 mL) was layered carefully with water/ethanol (1:1, 4 mL) and then an ethanol solution (3 mL) of $Cu(Ac)_2\cdot H_2O$ (0.013 g, 0.05 mmol). Slow diffusion at room temperature yielded green crystals of **1** in 2 weeks. Yield: 55% based on copper. Elem anal. Calcd for $C_{12}H_8O_2N_4Cu$: C, 47.45; H, 2.65; N, 18.44. Found: C, 47.58; H, 2.93; N, 18.87. Main IR bands (KBr, cm^{-1}): 2056(s) [$\nu(N_3)$], 1597(m) [ν_{as}(COO)], 1544(m), 1376(s) [ν_s(COO)], 1266(w).

$[Cu_2(4,4\text{-pybz})_3(N_3)]_n\cdot 3nH_2O$ (2). In a test tube, a dimethyl sulfoxide (DMSO) solution (3 mL) of 4,4-Hpybz (0.010 g, 0.05 mmol) and NaN_3 (0.013 g, 0.2 mmol) was layered carefully with DMSO/methanol (2:1, 3 mL) and then a methanol solution (3 mL) of $Cu(ClO_4)_2\cdot 6H_2O$ (0.013 g, 0.05 mmol). Slow diffusion at room temperature yielded green crystals of **2** in 1 week. Yield: 60% based on copper. Elem anal. Calcd for $C_{36}H_{30}O_9N_6Cu_2$: C, 52.88; H, 3.70; N, 10.28. Found: C, 52.89; H, 3.43; N, 9.99. Main IR bands (KBr, cm^{-1}): 2081(m) [$\nu(N_3)$], 1608(s) [ν_{as}(COO)], 1564(m), 1400(s) [ν_s(COO)], 1373(m).

$[Mn(4,4\text{-pybz})(N_3)(H_2O)_2]_n$ (3). A mixture of $MnCl_2\cdot 4H_2O$ (0.020 g, 0.1 mmol), NaN_3 (0.052 g, 0.8 mmol), and 4,4-Hpybz (0.005 g, 0.025 mmol) in DMSO (1 mL), methanol (1 mL), and distilled water (0.5 mL) was stirred for 30 min in air and then heated in a 23 mL Teflon-lined autoclave at 70 °C for 5 days. After the mixture was slowly cooled to room temperature, yellow block crystals of **3** were collected. Yield: 22% based on manganese. Elem anal. Calcd for $C_{12}H_{12}O_4N_4Mn$: C, 43.52; H, 3.65; N, 16.92. Found: C, 43.85; H, 3.91; N, 16.93. Main IR bands (KBr, cm^{-1}): 2089(m) [$\nu(N_3)$], 2063(s) [$\nu(N_3)$], 1607(s) [ν_{as}(COO)], 1558(m), 1381(s) [ν_s(COO)], 1009(w).

Table 1. Crystal Data and Structure Refinement for Compounds 1−3

	1	2	3
formula	$CuC_{12}H_8N_4O_2$	$Cu_2C_{36}H_{30}N_6O_9$	$MnC_{12}H_{12}N_4O_4$
M_r	303.76	817.76	331.20
cryst syst	monoclinic	monoclinic	monoclinic
space group	$P2_1$	$P2_1/c$	$P2_1/c$
a [Å]	8.5221(6)	15.2793(12)	11.3620(3)
b [Å]	6.4754(4)	19.3066(16)	15.3393(4)
c [Å]	11.5083(8)	20.7718(16)	7.5356(2)
β [deg]	108.673(2)	99.010(3)	90.0090(10)
V [Å^3]	601.64(7)	6051.9(8)	1313.34(6)
Z	2	4	4
ρ_{calcd} [g cm^{-3}]	1.677	0.897	1.675
μ [mm^{-1}]	1.817	0.740	1.028
no. of unique reflns	2744	13 054	3189
R_{int}	0.0383	0.0255	0.0254
R1 [$I > 2\sigma(I)$]	0.0470	0.0485	0.0264
wR2 (all data)	0.1126	0.1457	0.0732

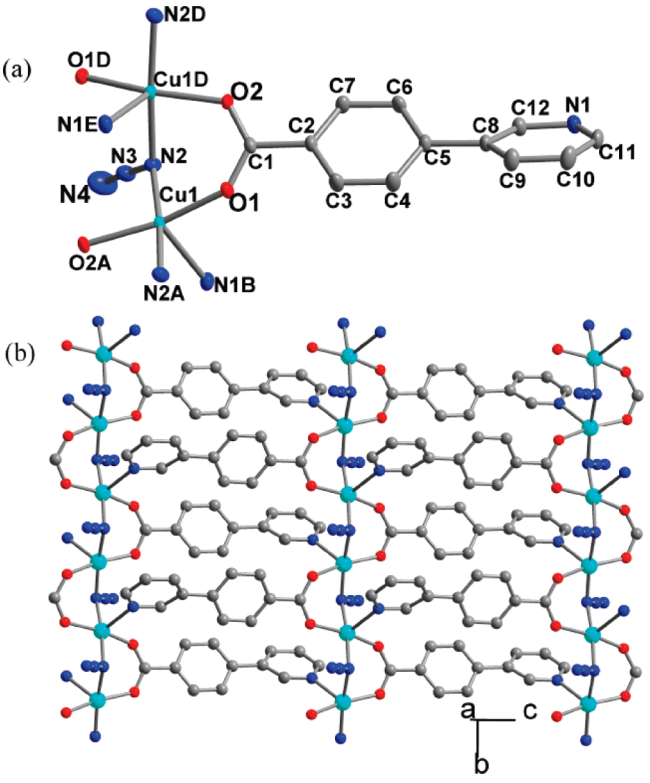

Figure 1. (a) Local coordination environments in compound **1**. Hydrogen atoms are omitted for clarity. (b) 2D network formed by the 4,3-pybz ligands connecting the copper−azide−carboxylate chains.

X-ray Crystallography. Diffraction data for **1**−**3** were collected at 296 K on a Bruker Apex II CCD area detector equipped with graphite-monochromated Mo Kα radiation (λ = 0.710 73 Å). Empirical absorption corrections were applied using the *SADABS* program.[21] The structures were solved by direct methods and refined by a full-matrix least-squares method on F^2, with all non-hydrogen atoms refined with anisotropic thermal parameters.[22] All of hydrogen atoms attached to

dx.doi.org/10.1021/ic2008842 |*Inorg. Chem.* 2011, 50, 7284–7294

Table 2. Selected Bond Lengths (Å) and Angles (deg) for Compound 1[a]

Cu1−O1	1.962(2)	Cu1−O2A	1.963(2)
Cu1−N2	1.985(3)	Cu1−N2A	1.994(3)
Cu1−N1B	2.320(3)		
O1−Cu1−O2A	166.55(11)	O1−Cu1−N2	90.85(11)
O2A−Cu1−N2	88.79(10)	O1−Cu1−N2A	88.83(11)
O2A−Cu1−N2A	89.61(11)	N2−Cu1−N2A	171.75(10)
O1−Cu1−N1B	92.65(10)	O2A−Cu1−N1B	100.79(10)
N2−Cu1−N1B	93.93(10)	N2A−Cu1−N1B	94.31(11)
Cu1−N2−Cu1D	109.40(12)		

[a] Symmetry codes: A, $-x+1, y-{}^1/_2, -z+2$; B, $-x+1, y+{}^1/_2, -z+1$; C, $-x+1, y-{}^1/_2, -z+1$; D, $-x+1, y-{}^1/_2, -z+2$.

carbon atoms were placed in calculated positions and refined using the riding model. The water hydrogen atoms in **3** were located from difference maps. In **2**, the uncoordinated guest molecules could not be modeled because of the heavy disorder and the limited quality of the data set. The final refinements were carried out using the data obtained by the *SQUEEZE* routine in the *PLATON* software package.[23] According to elemental analytical data, the guest molecules were proposed to be H_2O. Some 4,4-pybz ligands are also disordered. A summary of the crystallographic data, data collection, and refinement parameters is provided in Table 1.

RESULTS AND DISCUSSION

Description of the Structures. *Compound* ***1***. This compound contains a 2D coordination network in which 1D $[Cu(N_3)(COO)]_n$ chains are linked by the organic 4,3-pybz ligands (Figure 1a). Selected bond lengths and angles are listed in Table 2. The asymmetric unit consists of one metal ion, one 4,3-pybz, and one azide ion. The Cu^{II} ion exhibits a distorted square-pyramidal geometry, for which the basal plane consists of two carboxylate oxygen atoms and two azide nitrogen atoms with the apical position occupied by a pyridine nitrogen atom. The apical Cu−N distance [2.320(3) Å] is significantly longer than the basal Cu−N/O distances [1.962(2)−1.994(3) Å]. The distortion parameter τ, defined as $(\varphi_1 - \varphi_2)/60$ (φ_1 and φ_2 are the two largest bond angles of the coordination sphere) by Addison et. al.,[24] is 0.07, suggesting a basically square-pyramidal coordination geometry (τ = 0 and 1 for perfect square and trigonal bipyramids, respectively). The basal atoms deviate from their mean plane by less than 0.053(5) Å, and Cu1 is out of the mean basal plane by 0.1916(6) Å. Adjacent Cu^{II} ions are doubly linked by an azide bridge in the EO mode and a carboxylate bridge in the syn−syn mode to generate a uniform chain running along the *b* direction (Figure 1b). It is notable from the viewpoint of magnetic relevance that both bridges adopt the basal−basal disposition (the donor atoms of the bridges are at basal positions around metal ions). The Cu···Cu distances spanned by the double bridge are 3.248(1) Å, and the Cu−N−Cu angle is 109.4(1)°.

The 4,3-pybz ligands bind metal ions in the μ_3-tridentate coordination mode via the pyridyl and syn−syn carboxylate groups and thus interlink the $[Cu(N_3)(COO)]_n$ chains to generate a 2D layer along the *bc* plane (Figure 1b). The nearest interchain Cu···Cu distance is 11.508(1) Å, spanned by the ligand. The layers are packed with weak interlayer hydrogen bonds, which involve C−H groups from one layer and azide nitrogen atoms from another layer (see the Supporting Information, Figure S1). The shortest interlayer Cu···Cu distances are 8.522(1) Å.

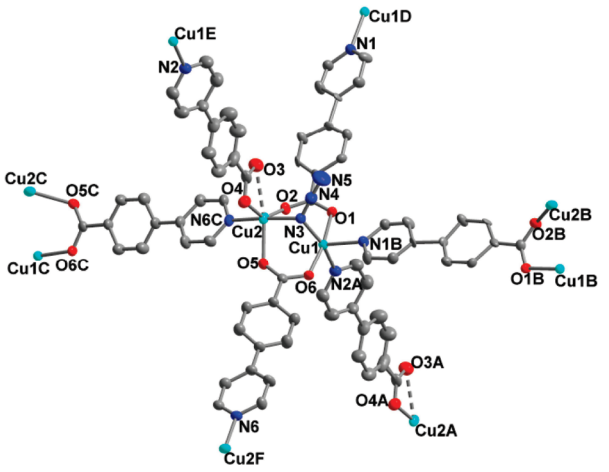

Figure 2. Coordination environments of Cu^{II} ions in compound **2** (30% probability thermal ellipsoids). For clarity, all hydrogen atoms are omitted.

Table 3. Selected Bond Lengths (Å) and Angles (deg) for Compound 2[a]

Cu1−O6	1.9190(17)	Cu1−O1	1.9469(17)
Cu1−N2A	2.032(3)	Cu1−N3	2.039(3)
Cu1−N1B	2.188(2)	Cu2−N3	1.953(2)
Cu2−O4	1.955(7)	Cu2−N6C	1.985(2)
Cu2−O2	2.174(2)	Cu2−O5	2.195(2)
O6−Cu1−O1	171.30(8)	O6−Cu1−N2A	89.72(10)
O1−Cu1−N2A	91.32(10)	O6−Cu1−N3	88.11(9)
O1−Cu1−N3	88.61(9)	N2A−Cu1−N3	164.62(10)
O6−Cu1−N1B	95.87(9)	O1−Cu1−N1B	92.53(9)
N2A−Cu1−N1B	98.31(11)	N3−Cu1−N1B	97.05(10)
N3−Cu2−O4	93.72(18)	N3−Cu2−N6C	172.68(11)
O4−Cu2−N6C	93.60(18)	N3−Cu2−O2	88.38(9)
O4−Cu2−O2	144.1(2)	N6C−Cu2−O2	85.82(9)
N3−Cu2−O5	86.64(9)	O4−Cu2−O5	105.9(2)
N6C−Cu2−O5	91.14(9)	O2−Cu2−O5	110.04(8)
Cu1−N3−Cu2	101.11(11)		

[a] Symmetry codes: A, $x-1, y, z$; B, $x, -y+{}^1/_2, z+{}^1/_2$; C, $x, -y+{}^3/_2, z-{}^1/_2$; D, $x, -y+{}^1/_2, z-{}^1/_2$; E, $x+1, y, z$; F, $x, -y+{}^3/_2, z+{}^1/_2$.

Compound ***2***. According to X-ray crystallographic analyses, the structure is a 3D metal−organic framework based on dinuclear units with mixed azide and carboxylate bridges. The unit structure is shown in Figure 2, and selected bond lengths and angles are listed in Table 3. There are two Cu^{II} ions in the asymmetric unit. The Cu1 ion resides in a distorted square-pyramidal environment: the basal plane defined by two carboxylate oxygen atoms (O1 and O6), an azide nitrogen atom (N3), and a pyridyl nitrogen atom (N2A). The apical position is occupied by another pyridyl nitrogen atom (N1B), with the apical Cu−N distance [ca. 2.188(2) Å] being longer than the basal Cu−O/N distances [1.919(2)−2.039(3) Å]. The basal atoms deviate from their mean plane by less than 0.098(3) Å, and Cu1 is out of the mean basal plane by 0.186(3) Å. The trigonality index for this Cu site has been calculated to be τ = 0.11, suggesting a square-pyramidal geometry with very slight distortion. Differently, the coordination surrounding of Cu2 is intermediate

dx.doi.org/10.1021/ic2008842 |*Inorg. Chem.* 2011, 50, 7284–7294

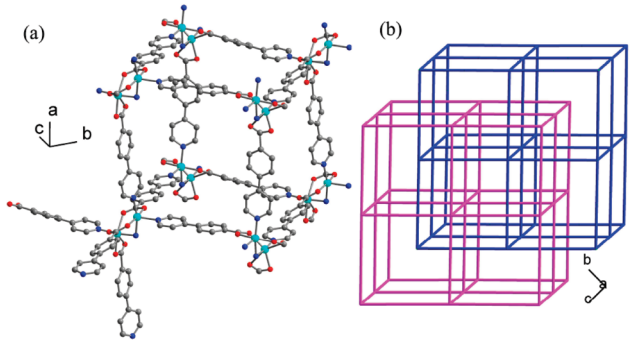

Figure 3. (a) Single **pcu** net based on dinuclear units in **2**. (b) 2-fold interpenetration of the nets.

between square-pyramidal and trigonal-bipyramidal, with τ = 0.48. For a square-pyramidal description, the basal plane, similar to that for Cu1, consists of two carboxylate oxygen atoms (O2 and O4), an azide nitrogen atom (N3), and a pyridyl nitrogen atom (N6C), but the apical position is completed by a third carboxylate oxygen atom (O5). The axial Cu2−O5 distance [2.195(2) Å] is slightly longer than the basal Cu2−O2 distance [2.174(2) Å] and significantly elongated compared with the other basal Cu−O/N distances [1.953(2)−1.985(2) Å]. For the trigonal-bipyramidal description, the equatorial plane is defined by three carboxylate oxygen atoms, with two axial nitrogen atoms from azide and pyridyl. We noted that a fourth carboxylate oxygen atom (O3) is at 2.568(2) Å from Cu2, suggesting weak coordination. If this is included, the O4−C−O3 carboxylate binds Cu2 in a highly asymmetric chelating fashion with a small bit angle of 54.3(3)°, and the geometry around Cu2 may be described as a highly distorted octahedral.

Cu1 and Cu2 is triply bridged by an EO azide and two syn−syn carboxylates to generate a dinuclear $[Cu_2(N_3)(COO)_2]$ motif. The Cu···Cu distance is 3.083(3) Å, with Cu−N−Cu = 101.1(1)°. Noticeably, both the distance and the bridging angle are the smallest of the known copper(II) complexes with mixed azide and carboxylate bridges (see below). Assuming a square-pyramidal geometry for both metal ions, the basal planes of Cu1 and Cu2 are almost orthogonal to each other with a dihedral angle of 89.33(7)°. The azide and O1−C−O2 bridges are in the basal−basal fashion, while the O5−C−O6 carboxylate bridge adopts the apical−basal disposition (O5 at the apical position of Cu2 and O6 at the basal position of Cu1). These features are pertinent to the magnetic properties.

The dimeric unit is furnished by six 4,4-pybz ligands, which radiate in octahedral directions and adopt μ_3- or μ_2-tridentate coordination modes (with bridging or asymmetrically chelating carboxylate groups, respectively). Thus, the units serve as six-connecting octahedral secondary building units to yield a 3D metal−organic framework, which has the topology of the primitive cubic (**pcu**, or α-Po) net (Figure 3a). The shortest interdimeric Cu···Cu distances along the three independent 4,4-pybz ligands are 13.065(4), 13.144(4), and 13.160(1) Å. The long spacer between the dimeric nodes results in large open cavities within a single net, which is partially filled via 2-fold interpenetration (Figure 3b). Weak hydrogen bonds are observed between two sets of interpenetrating structures, which involve a pyridine C−H group from one set and the carboxylate O3 atom from the other set (Figure S2 in the Supporting Information). The shortest Cu···Cu distance between the two

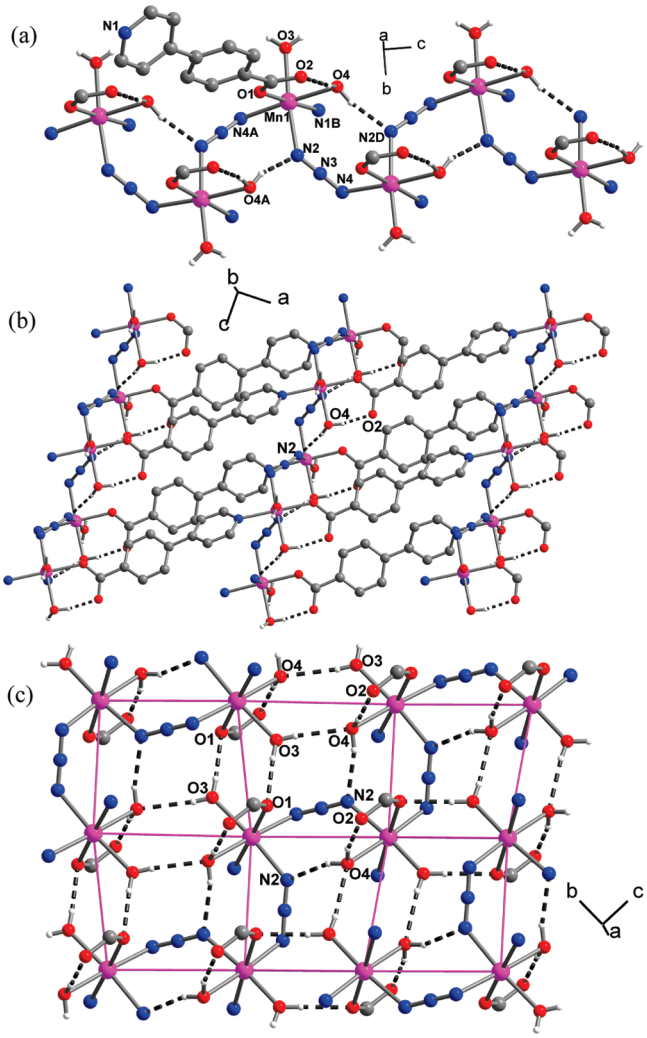

Figure 4. Structure of **3**: (a) a chain with azide and hydrogen-bonding bridges; (b) a top view of the 2D layer formed by 4,4-pybz interlinking the chains; (c) a 2D sheet through hydrogen bonds. The purple lines highlight the 4^4 net topology. Parameters for hydrogen bonds: O4−H4B···O2 = 164.7(2)°, H···O = 1.79(2) Å, and O4···O2 = 2.605(2) Å; O4−H4C···N2 (x, 1.5 − y, 0.5 + z) = 159.6(2)°, H···N = 2.08(2) Å, and O4···N2 = 2.870(2) Å.

nets is 7.489(6) Å. The cavities left in the 2-fold interpenetrated structure are occupied by water molecules.

Compound ***3***. Single-crystal X-ray analyses revealed that the structure of compound **3** contains 2D coordination layers in which 1D $[Mn(EE\text{-}N_3)]_n$ chains are interlinked by the 4,4-pybz ligands (Figure 4a). Selected bond distances and angles are given in Table 4. The unique Mn1 ion assumes a distorted octahedral geometry completed by two azide nitrogen atoms (N2 and N4A), a carboxylate oxygen atom (O1), a pyridyl nitrogen atom (N1B), and two water molecules (O3 and O4). The average bond lengths are 2.232(1) Å for Mn−N and 2.200(1) Å for Mn−O. The bond valence sum[25] is 1.999, indicating the Mn^{II} oxidation state (this is also supported by magnetic data; see below). Adjacent metal ions are bridged by single end-to-end (EE) azide ligands, with a Mn···Mn distance of 5.338(1) Å, to generate a uniform chain along the c direction, with a zigzag arrangement of manganese ions. Coordination of the azide bridge is asymmetric, as shown by Mn1−N2−N3 = 130.1(1)° and Mn1A−N4−N3 = 117.8(1)°.

dx.doi.org/10.1021/ic2008842 |*Inorg. Chem.* 2011, 50, 7284–7294

Table 4. Selected Bond Lengths (Å) and Angles (deg) for Compound 3[a]

Mn1−O1	2.1572(10)	Mn1−O3	2.1753(12)
Mn1−N4A	2.2168(14)	Mn1−N1B	2.2341(12)
Mn1−N2	2.2455(14)	Mn1−O4	2.2682(11)
O1−Mn1−O3	87.63(4)	O1−Mn1−N4A	87.17(5)
O3−Mn1−N4A	99.64(5)	O1−Mn1−N1B	178.57(4)
O3−Mn1−N1B	90.97(5)	N4A−Mn1−N1B	93.32(5)
O1−Mn1−N2	91.40(5)	O3−Mn1−N2	172.76(5)
N4A−Mn1−N2	87.47(5)	N1B−Mn1−N2	89.96(5)
O1−Mn1−O4	90.60(4)	O3−Mn1−O4	83.35(4)
N4A−Mn1−O4	176.19(5)	N1B−Mn1−O4	88.98(4)
N2−Mn1−O4	89.49(5)		

[a] Symmetry codes: A, x, $-y + {}^3/_2$, $z - {}^1/_2$; B, $x - 1$, y, $z + 1$; C, $x + 1$, y, $z - 1$; D, x, $-y + {}^3/_2$, $z + {}^1/_2$.

The Mn−N_3−Mn torsion angle, defined by the dihedral angle between the Mn1−N2−N3−N4 and Mn1A−N4−N3−N2 planes, is 74.5(1)°, defining a gauche conformation for the Mn−N_3−Mn bridging moiety.

The 4,4-pybz ligand with monodentate carboxylate and pyridyl groups interlinks the $[Mn(EE\text{-}N_3)]_n$ chains into a 2D network (Figure 4b). The zigzag chains are aligned and linked in a shoulder-by-shoulder fashion so that the 2D network looks like a bilayer structure as revealed by a side view shown in Figure S3 in the Supporting Information. The ligand separates the manganese ions by 13.635(6) Å, while the shortest interchain Mn···Mn distance within the layer is 11.362(1) Å.

The layers are packed in parallel into the 3D structure. Two sets of hydrogen bonds are formed with coordinated water molecules as donors (Figure 4c). One set is along the azide-bridged chain, involving the O4 water molecule. The O4−H···O2 interaction stabilizes the monodentate coordination of the carboxylate group by generating a six-membered ring, while the O4−H···N2 interaction reinforces the chain structure by providing a triatomic hydrogen-bonding bridge between neighboring Mn^{II} ions. The other set is between the azide-bridged chains from different layers, involving the O3 water molecules. The intra- and interchain hydrogen bonds collaborate with the azide coordinative bridges to arrange the manganese spheres into a square-grid-like 2D sheet along the *bc* plane, in which manganese atoms are linked by triatomic N−N−N and O−H···O/N bridges. The Mn···Mn distance spanned by the (N−N−N)-(O4−H···N2) bridges is 5.338(1) Å, and those by the $(O3-H\cdots O4)_2$ and $(O3-H\cdots O1)_2$ bridges are 6.105(1) and 5.259(1) Å, respectively. It is noted that the last distance associated with double hydrogen bonds is even shorter than that spanned by the coordinative azide bridge. Considering this hydrogen-bonded layer with short metal-to-metal distances, the whole structure of **3** may be described as a layer-pillared 3D network, with the 4,4-pybz ligands as pillars (Figure S4 in the Supporting Information).

Magnetic Properties. *Complex* ***1***. The susceptibility (χ) of compound **1** was measured under 1 kOe in the 2−300 K range (Figure 5). The χT value per Cu^{II} at room temperature is about 0.519 emu K mol^{-1}, higher than the value expected for a magnetically isolated Cu^{II} ion. As the temperature is lowered, the χ and χT values increase smoothly to maxima at 5.9 and 10 K, respectively, and then decrease rapidly. The data above 150 K follow the

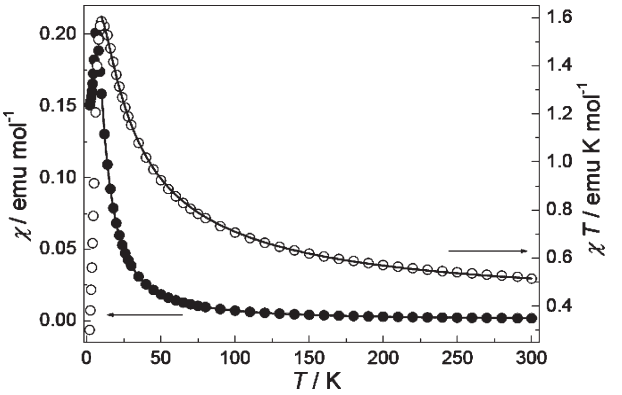

Figure 5. Temperature dependence of χT and χ for **1** under 1 kOe. The solid lines represent the best fit to the appropriate model (see the text).

Curie−Weiss law with C = 0.44 cm^3 K mol^{-1} and θ = 44.0 K. The positive θ value suggests the presence of dominant ferromagnetic coupling between Cu^{II} ions.

Magnetically, the system can be treated as a uniform chain in which magnetic exchange is mediated through the $(COO)(N_3)$ double bridge. The susceptibility expression proposed by Baker et al. for Heisenberg ferromagnetic $S = {}^1/_2$ chains (eq 1)[26] and the molecular-field approximation accounting for interchain interactions (eq 2)[27] were used for magnetic analysis with A = 1 + 5.7979916x + 16.902653x^2 + 29.376885x^3 + 29.832959x^4 + 14.036918x^5 and B = 1 + 2.7979916x + 7.008678x^2 + 8.6538644x^3 + 4.5743114x^4 and where $x = J/2kT$ based on the spin Hamiltonian $\boldsymbol{H} = -J\Sigma S_i S_{i+1}$.

$$\chi_{chain} = \frac{Ng^2\beta^2}{4kT}\left(\frac{A}{B}\right)^{2/3} \quad (1)$$

$$\chi = \frac{x_{chain}}{1 - (zJ'x_{chain}/Ng^2\beta^2)} \quad (2)$$

The experimental susceptibility data above 10 K have been best fitted by the above expressions with best-fit parameters J = 63.9 cm^{-1}, g = 2.06, and zJ' = −2.31 cm^{-1} (zJ' describes the interchain antiferromagnetic interaction). The positive J value confirms the ferromagnetic coupling through the $(COO)(N_3)$ double bridge.

The small negative zJ' value indicates the presence of interchain antiferromagnetic interactions, consistent with the drop of the χT product at low temperature. The drop of χ at further lower temperature may indicate the occurrence of long-range antiferromagnetic ordering. To further investigate the low-temperature behavior, the field-cooled (FC) magnetizations under different fields were measured and are shown in Figure 6a. At 5.0 kOe, the M versus T curves display a maximum at 5.2 K, consistent with the antiferromagnetic ordering. As the field is lifted, the maximum shifts toward lower temperatures, becomes less prominent, and finally disappears at a high field of 9.0 kOe. The FC behaviors are characteristic of field-induced metamagnetism,[28] with the disappearance of the maximum indicating that the interchain antiferromagnetic ordering is broken up by the field.

The antiferromagnetic ordering is confirmed by the alternating-current thermal susceptibility measured under a zero direct-current field (Figure S5 in the Supporting Information), which

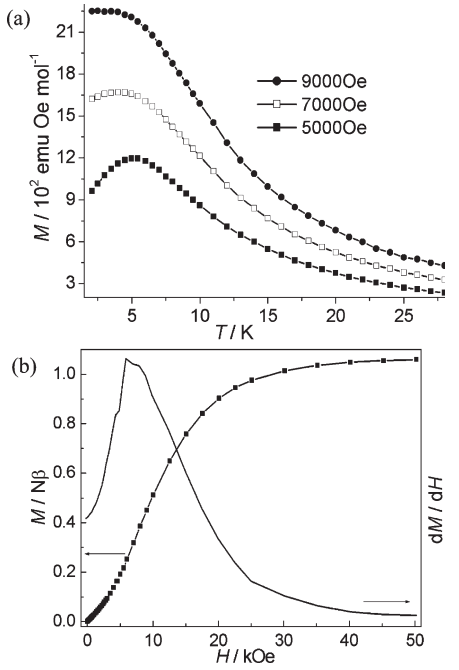

Figure 6. (a) FC magnetization curves for **1** at different fields. (b) Isothermal magnetization curves at 2 K for **1**.

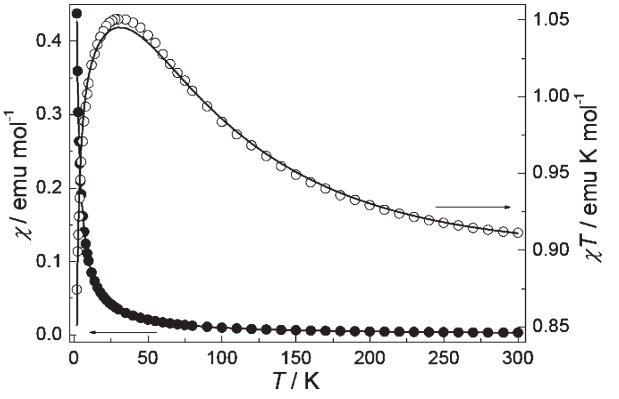

Figure 7. Temperature dependence of χ and χT for **2** under 1 kOe. The solid lines represent the best fit using eqs 2 and 3 (see the text).

exhibits a frequency-independent maximum in the real component (χ') at 6.2 K with zero imaginary signals (χ''). Metamagnetism is confirmed by the sigmoidal shape of the isothermal magnetization curve measured at 2 K, and the critical field is estimated to be H_c = 6.1 kOe according to the dM/dH plot (Figure 6b). The slow increase of magnetization at $H < H_C$ is consistent with antiferromagnetic ordering, while the rapid increase toward saturation at high field is consistent with a ferromagnetic state. These features indicate a spin−flip transition, for which the anisotropy field is larger than the interchain exchange field.[29] No evident hysteresis was observed upon cycling of the field between −3 and 3 T at 2 K (Figure S6 in the Supporting Information).

Complex **2**. The susceptibility (χ) of complex **2** was measured under 1 kOe in the 2−300 K range and is shown as χT and χ vs T plots in Figure 7. The χT value per dimer at room temperature is about 0.91 emu K mol^{-1}, higher than the spin-only value expected for two uncoupled $S = {}^1/_2$ spins. As the temperature is lowered, the product increases to a maximum of 1.05 emu mol^{-1} K at 29.7 K and then decreases rapidly, while the χ value increases monotonically. The data above 100 K follow the Curie−Weiss law with C = 0.88 cm^3 K mol^{-1} and θ = 11.3 K. The high-temperature behavior suggests an intradimeric ferromagnetic coupling, while the low-temperature decrease in χT is attributable to interdimeric antiferromagnetic interactions and/or zero-field splitting (ZFS). FC and zero-field-cooled (ZFC) magnetization measurements were performed over the temperature range 2−24 K under a low field of 10 Oe (Figure S7 in the Supporting Information). The FC and ZFC data do not show divergence, and the magnetization increases continuously with decreasing temperature; no maximum was observed. These observations indicate the absence of any long-range magnetic ordering.

To evaluate the interactions, the magnetic behavior of the dinuclear unit can be simulated with the modified Bleaney−Bowers equation[30] based on the Hamiltonian $\boldsymbol{H} = -JS_1 \cdot S_2$:

$$\chi_{\text{dimer}} = \frac{2Ng^2\beta^2}{kT[3 + exp(-J/kT)]} \qquad (3)$$

To get a better fit over the whole temperature range, the molecular-field approximation (eq 2, replacing χ_{chain} with χ_{dimer}) was applied for the interdimeric interactions (zJ') and the temperature-independent paramagnetism was assumed to be 120 × 10^{-6} emu mol^{-1} per dimer. The best fit led to J = 93.6 cm^{-1}, g = 2.06, and zJ' = −0.52 cm^{-1}. The positive J value confirms a strong intradimeric ferromagnetic interaction through the $(COO)_2(N_3)$ triple bridge, while the negative zJ' value suggests interdimeric antiferromagnetic coupling.

Alternatively, considering the ZFS within the S = 1 ground state, which is conventionally assumed to be axial, the magnetic susceptibility for the dimer can be expressed as[1a]

$$\chi_{\text{dimer}} = \frac{2x_\perp + x_\parallel}{3} \qquad (4)$$

with $\chi_\parallel = 2Ng^2\beta^2[\exp(-D/3kT)]/kT[\exp(2D/3kT) + 2\exp(-D/3kT) + \exp(-J/kT)$ and $\chi_\perp = 2Ng^2\beta^2[\exp(2D/3kT) - \exp(-D/3kT)/D[\exp(2D/3kT) + 2\exp(-D/3kT) + \exp(-J/kT)]$. The fit of the experimental data to eq 4 with J, g, and D parameters failed to give satisfactory agreement. When both D and zJ' are included by combining eqs 2 and 4, the best fit gave J = 96.1 cm^{-1}, g = 2.06, and zJ' = −0.52 cm^{-1} with a negligible D value (0.0004 cm^{-1}). The J, g, and zJ' values are nearly the same as those obtained using eqs 2 and 3. These results should suggest that antiferromagnetic interactions are indeed operative between dimers and are the main reason for the observed χT decrease at low temperature.

We have described two new copper(II) compounds with simultaneous azide and carboxylate bridges: **1** with (EO-N_3)-(COO) double bridges and **2** with (EO-N_3)$(COO)_2$ triple bridges. To our knowledge, compound **2** is thus far the only copper(II) species with (EO-N_3)$(COO)_2$ triple bridges, which have been observed in several manganese(II) and cobalt(II) compounds.[18] Despite the remarkable differences in their bridging multiplicity, coordination network, and bulk magnetic behaviors, both compounds show ferromagnetic coupling through simultaneous bridges. As has been noted, one of the carboxylate bridges in **2** adopts the basal−apical disposition between square-pyramidal Cu^{II} ions. Because a Cu^{II} ion in the usual square-planar (sp), square-pyramidal (spy), or axially elongated octahedral

dx.doi.org/10.1021/ic2008842 |*Inorg. Chem.* 2011, 50, 7284–7294

Table 5. Structural and Magnetic Parameters for Equatorial−Equatorial (Basal−Basal) Carboxylate and EO-Azide Bridges in Copper(II) Complexes

complex[a]	axial−axial bridge	Cu−N−Cu (deg)	Cu···Cu (Å)	τ^b	J (cm^{-1})[c]	ref
$[Cu_{1.5}(N_3)_2(isonic)]_n$		106.7	3.20	0.11	80	19d
$[Cu_{1.5}(hnta)(N_3)_2(H_2O)]_n$	μ-O_{water}	103.2	3.12	0.22	89	35a
$[Cu_3(hnta)_4(N_3)_2(H_2O)_3]_n$		116.2	3.39	0.29	69.7	35a
$[Cu(N_3)(L^1))(DMSO)]_n$	μ-O_{DMSO}	106.5	3.19	Oct	126	35b
$[Cu_3(N_3)_4(L^1)_2(DMSO)_2]_n$	μ-O_{DMSO}	107.6	3.22	0.11	126	35b
$[Cu_2(N_3)_2(NO_3)_2(L^2)_2]_n$	μ-1,3-NO_3	119.5	3.44	Oct	26	35c
$\{[Cu(Hpht)(N_3)].H_2O\}_n$		111.9	3.28	Oct	75	35d
$[Cu(INO)(N_3)(H_2O)_{0.5}]_n$	μ-$O_{carboxylate}$	106.6	3.22	Oct	80	35e
$[Cu(NNO)(N_3)(H_2O)_{0.5}]_n$		124.3	3.52	0.22	48	35e
$[Cu(benzoate)(N_3)]_n$		126.8	3.54	Sp	33.9	16c
$[Cu(L^3)(N_3)]_n$	μ-1,1-N_3	108.2	3.23	Oct	93.1	16c
$[Cu(1\text{-naphthoate})(N_3)]_n$		116.9	3.41	Oct	65.6	16c
$[Cu(N_3)(tp)(CH_3OH)]_n$	μ-O_{MeOH}	105.5	3.19	Oct	63	35f
$[Cu(N_3)(nic)]_n$		113.6	3.35	0.54	39.1	19b
$[Cu(N_3)(p\text{-CPA})]_n$		107.0	3.18	0.13	68.8	35g
$[Cu(4,3\text{-pybz})(N_3)]_n$		109.4	3.25	0.01	63.9	this work
$[Cu_2(4,4\text{-pybz})_3(N_3)]_n \cdot 3nH_2O$	μ-COO	101.1	3.08	0.11	96.1	this work
				0.48		

[a] Isonic = isonicotinate, hnta = 6-hydroxynicotinate, L^1 = $\mu_{1,3}$-($C_4H_3SCH_2COO$), L^2 = $Me_3NCH_2CO_2$, Hpht = hydrogen phthalate, INO = isonicotinate *N*-oxide, NNO = nicotinate *N*-oxide, L^3 = 2-methylbenzoate, tp = terephthalate; 4,3-pybz = 4-(3-pyridyl)benzoate; 4,4-pybz = 4-(4-pyridyl)benzoate, nic = nicotinate, *p*-CPAH = *p*-cyanophenoxyacetic acid. [b] The geometric parameter describes the distortion of square-pyramidal coordination toward trigonal-bipyramidal. This is not applicable to octahedral and square-planar geometry. Oct = octahedral, Sp = square planar. [c] All of the J values were quoted using the Hamiltonian $\boldsymbol{H} = -JS_1 \cdot S_2$.

(oct) environment features a $d_{x^2-y^2}$-type magnetic orbital delocalized toward basal (or equatorial) ligands from Cu^{II} with negligible delocalization toward apical (or axial) ligands, the basal−apical carboxylate bridge in **2** is a poor pathway for magnetic exchange and may be neglected (it can be assumed that the additional basal−apical bridge may influence magnetic exchange in an indirect way, for instance, by altering the bridging parameters of the basal−basal bridges). Thus, the effective exchange pathways in **2** are similar to those in **1**, including two dissimilar basal−basal bridges: a syn−syn carboxylate and an EO azide.

While the syn−syn carboxylate bridge in the basal−basal (or equatorial−equatorial, eq−eq) disposition always induces antiferromagnetic exchange between Cu^{II} ions,[10a] the exchange through basal−basal (or eq−eq) EO-azide bridges is sensitive to the Cu−N−Cu angle, with a crossover from ferro- to antiferromagnetic as the angle increases across 108° according to empirical analyses[31] or 104° according to a density functional theory study.[32] However, the crossover angle is not valid for systems with simultaneous azide and carboxylate bridges, and the overall interaction is not the simple addition of contributions from two individual bridges. Ferromagnetic coupling has been observed for mixed-bridged systems with large Cu−N−Cu angles, which are expected to induce antiferromagnetic coupling in the absence of carboxylate. This has been justified by orbital countercomplementarity:[1a,33] the incorporation of the carboxylate bridge reduces the energy gap between the two singly occupied molecular orbitals in the triplet state and hence diminishes (i.e., counterbalances) the antiferromagnetic contribution, leading to overall ferromagnetic coupling ($J = J_F + J_{AF} > 0$ when $|J_{AF}| < J_F$).

To deduce general magnetostructural information for the simultaneous basal−basal (or eq−eq) azide and carboxylate bridges, the structural and magnetic data for relevant copper(II) complexes are collected in Table 5. Note that some of these compounds have a third bridge ($\mu_{1,3}$-NO_3, μ-EO-N_3, or μ-O) at apical (or axial) positions around Cu^{II} ions, which has little contribution to magnetic exchange. The compounds with simultaneous azide and carboxylate bridges but with one or both of the bridges in axial positions[34] are not included in the collection for their evidently different magnetic properties.

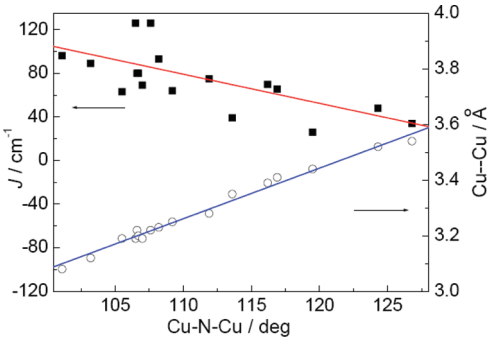

Figure 8. J and Cu···Cu distances against the bridging Cu−N−Cu angle. The solid lines are just guides for the eye.

As can be seen from Table 5, all of the copper(II) compounds with simultaneous bridges exhibit ferromagnetic interactions, independent of the Cu−N−Cu angle in the wide range of 101−127°. While no evident correlations can be deduced between the J values and the structural parameters of the carboxylate bridges, the magnitude of the interaction seems to be mainly dependent upon the azide bridge. The J values are plotted against the Cu−N−Cu angles in Figure 8. A general trend is evident that the ferromagnetic interaction decreases as

dx.doi.org/10.1021/ic2008842 |*Inorg. Chem.* 2011, 50, 7284–7294

the bridging angle increases in the wide range from 101 to 127°. The fluctuations may be due to unidentified structural factors (for instance, the variations in the bridging mode of carboxylate) or experimental uncertainty.

There is also a general trend that J decreases with the Cu···Cu distance. This correlation is trivial because Cu···Cu is mainly determined by the Cu−N−Cu angle (note that the Cu−N distances for these compounds are very similar and vary in the narrow range of 1.96−2.01 Å). The Cu···Cu distances are also plotted against the Cu−N−Cu angles in Figure 8 to illustrate the linear increase of Cu···Cu with Cu−N−Cu.

We note that compound **2** has the smallest Cu−N−Cu angle and Cu···Cu distance among all of these mixed bridging systems, and the Cu2 coordination exhibits the largest distortion from square-pyramidal to trigonal-bipyramidal. Because Cu^{II} in the trigonal-bipyramidal field has an axial magnetic orbital (d_{z^2}) and the azide bridge in this compound lies at an axial position, the distortion does not prevent the azide bridge from being an efficient pathway for magnetic exchange.

Complex ***3***. The magnetic susceptibility of complex **3** was measured in the 2−300 K temperature range under 1 kOe (Figure 9). That measured at 300 K is about 3.83 emu K mol^{-1}, which indicates a high-spin Mn^{II} system with antiferromagnetic interactions and rules out the possibility of a Mn^{III} state (the spin-only values for high-spin Mn^{II} and Mn^{III} are 4.38 and 3.00 emu K mol^{-1}, respectively). Upon cooling, the χT value decreases monotonically, while the χ value increases to a broad maximum around 25 K and then increases rapidly upon further cooling below 10 K. The data above 110 K follow the Curie−Weiss law with C = 4.24 cm^3 K mol^{-1} and θ = −32.4 K. The above features

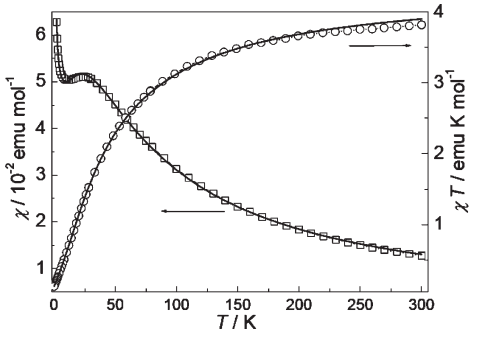

Figure 9. Temperature dependence of χ and χT for **3** under 1 kOe. The solid lines represent the best fit to the Fisher model (see the text).

indicate antiferromagnetic coupling between Mn^{II} ions. The rise in χ below 12 K may be due to the presence of a paramagnetic impurity.

According to the structural data, the Mn^{II} ions in **3** are linked into chains by EE-azide and O−H···N bridges and are further arranged in layers by two sets of double O−H···O bridges. Although all of the bridges are triatomic with comparable Mn···Mn separations, the magnetic interactions through the hydrogen-bonding pathways should be much weaker than those through covalent bridges.[36] Therefore, the system could be treated as a quasi-1D system. A uniform antiferromagnetic chain exhibits a characteristic susceptibility maximum at $kT_{max} \approx 0.5|J|S(S+1)$ (the Hamiltonian is $\boldsymbol{H} = -J\Sigma S_i S_{i+1}$),[37a] which indicates the short-range antiferromagnetic order along the chain. From this relationship, the intrachain exchange parameter of **3** (T_{max} = 25 K) could be estimated to be $J = -4.0$ cm^{-1}. To be more exact, the well-known classical-spin equation derived by Fisher has been used.[37b]

$$\chi_{chain} = \frac{Ng^2\beta^2 S(S+1)}{3kT}\frac{1+u}{1-u} \qquad (5)$$

where u is the Langevin function $u = \coth[JS(S+1)/kT] - kT/[JS(S+1)]$. The molecular-field approximation (eq 2) was applied to include the possible interchain interactions through hydrogen bonds, and a ρ parameter representing the molar fraction of the paramagnetic impurity [assumed to be mononuclear manganese(II) species, $\chi_{impurity} = 4.375/T$] has also been included to account for the observed rise in χ below 10 K. With $S = {}^5/_2$ and g fixed at 2.00, the best fit in the whole temperature range led to $J = -4.16$ cm^{-1}, $zJ' = 0.017$, and $\rho = 0.0098$. The J value confirms the antiferromagnetic interaction through a single EE-azide bridge, while the very small zJ' value indicates that the hydrogen bonds transmit weak interactions between Mn^{II} ions.

Alternatively, the numerical approach

$$\chi_{chain} = \frac{Ng^2\beta^2}{kT}\left(\frac{A+Bx^2}{1+Cx+Dx^3}\right) \qquad (6)$$

proposed by Weng[38a] has been used to fit the data, where $x = |J|/2kT$. The coefficients were determined by Hatfield et al. for antiferromagnetic $S = {}^5/_2$ chains: A = 2.9167, B = 208.04, C = 15.543, and D = 2707.2.[38b] The best fit of the experimental data by combining eqs 2 and 6 and a ρ parameter generated an unrealistically large zJ' value. When this parameter is ignored, a

Table 6. Structural and Magnetic Parameters for the Single EE-Azide Bridges in 1D Manganese(II) Complexes

complex[a]	Mn−N (Å)	Mn−N−N (deg)	Mn···Mn (Å)	Mn−N_3−Mn (deg)	J (cm^{-1})	ref
$\{[Mn(N_3)(dpyo)Cl(H_2O)_2](H_2O)\}_n$	2.21	127.6	6.13	180	−3.5	41a
	2.22	159.8	6.63	180	−0.12	
$[Mn(L^1)(N_3)PF_6]_n$	2.29	122.0	6.01	127	−4.8	41b
$[Mn(H_2O)(\mu\text{-}N_3)(N_3)(quinaz)_2]_n$	2.21	140.0	6.40	180	−4.4	41c
$[Mn_2(3\text{-}ampy)_4(\mu\text{-}N_3)_2(N_3)_2(H_2O)_2]_n$	2.24	136.7	6.35	165	−3.15	41d
$[Mn(R\text{-}L)_2(N_3)]_n(ClO_4)_n$	2.15	144.1	5.93	26.1	−4.7	41e
$[Mn(L^2)_2(N_3)]_n(ClO_4)_n$	2.18	142.8	5.97	86	−6.6	41f
$[Mn(N_3)_2(L^3)(CH_3OH)]_n$	2.21	146.0	6.03	0.7	−5.3	41g
$[Mn(4,4'\text{-}pybz)(N_3)(H_2O)_2]_n$	2.23	124.0	5.34	74.5	−4.15	this work

[a] dpyo = 4,4′-dipyridyl-*N*,*N*′-dioxide, quinaz = quinazoline, 3-ampy = 3-aminopyridine, L^1 = 2,13-dimethyl-3,6,9,12,18-pentaazabicyclo{12.3.1}-octadeca-1,(18),2,12,14,16-pentaene, R-L = (*R*)-pyridine-2-carbaldehyde-imine, L^2 = 4-methoxy-*N*-(pyridin-2-ylmethylene)aniline; L^3 = (1*E*,2*E*)-1,2-bis[phenyl(pyridin-4-yl)methylene)hydrazine, 4,4-pybz = 4-(4-pyridyl)benzoate.

dx.doi.org/10.1021/ic2008842 |*Inorg. Chem.* 2011, 50, 7284–7294

Scheme 1. Views Showing the Different Conformations of the Single EE-Azide-Bridged Mn−N_3−Mn Moiety

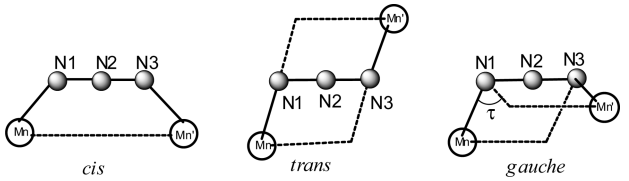

fairly good agreement has been obtained with $J = -3.89$ cm^{-1} and $\rho = 0.0111$ with $g = 2.00$. The J and ρ values are in good agreement with those obtained using eqs 2 and 5.

Several manganese(II) chains with single EE-azide bridges have been reported in the literature, all exhibiting antiferromagnetic interactions, as predicted for the bridge from extended Hückel molecular orbital calculations.[39] Some relevant structural and magnetic parameters are summarized in Table 6. The Mn−N_3−Mn torsion angle (τ) varies widely from about 0 to 180°, defining different conformations for the bridging moiety (Scheme 1): the (quasi-)planar cis and trans conformations ($\tau \sim 0$ and 180°, respectively) and the out-of-plane gauche conformation, with τ deviating significantly toward 90°. The other structural parameters vary in the ranges 2.15−2.29 Å for Mn−N, 122.0−159.8° for Mn−N−N, and 5.34−6.63 Å for Mn···Mn, while the J values vary in the large range from −0.12 to −6.6 cm^{-1}. No unambiguous magnetostructural correlations can be deduced from these data. More systematic studies are needed for such multifactorial systems, and besides the above-mentioned structural parameters, other factors, for instance, the imprint of the diverse nonbridging ligands upon magnetic orbitals, may also be important.[40]

CONCLUSION

We have described three copper(II) and manganese(II) coordination polymers with azide and two isomers of pyridylbenzoic acid, 4,3-Hpybz, and 4,4-Hpybz ligands. Diverse structures and magnetic properties have been observed. In compound **1**, the Cu^{II} ions are linked by mixed (μ-EO-N_3)(μ-COO) double bridges to give uniform chains, which are, in turn, linked into 2D layers by the 4,3-pybz ligands. Compound **2** exhibits 2-fold interpenetration of 3D frameworks based on [Cu_2(μ-EO-N_3)(μ-COO)$_2$] units. Compound **3** contains 2D manganese(II) coordination networks in which the chains with single μ-EE-N_3 bridges are interlinked by the 4,4-pybz ligands, and the structure also features a 2D hydrogen-bonded network in which Mn^{II} ions are linked by three kinds of double triatomic bridges, (μ-EE-N_3)(O−H···N), (O_{water}−H···O_{water})$_2$, and (O_{water}−H···$O_{carboxylate}$)$_2$. The magnetic properties of **3** are dominated by antiferromagnetic interactions through the EE-azide bridges along the chain. The simultaneous EO-azide and carboxylate bridges in **1** and **2** induce ferromagnetic coupling between Cu^{II} ions. A magnetostructural survey indicates a general trend that the ferromagnetic coupling through the mixed bridges decreases as the Cu−N−Cu angle increases. In addition, compound **1** exhibits antiferromagnetic ordering below 6.2 K and behaves as a field-induced metamagnet.

ASSOCIATED CONTENT

Supporting Information. Crystallographic information for compounds **1**−**3** in CIF format, supplementary structural graphics, $\chi'(T)$ and $\chi''(T)$ plots, isothermal magnetization, and ZFC and FC magnetization curves. This material is available free of charge via the Internet at http://pubs.acs.org.

AUTHOR INFORMATION

Corresponding Author

*E-mail: eqgao@chem.ecnu.edu.cn. Fax: +86-21-62233404.

ACKNOWLEDGMENT

This work was supported by the NSFC (Grant 20771038) and the Fundamental Research Funds for the Central Universities.

REFERENCES

(1) (a) Kahn, O. *Molecular Magnetism*; VCH: New York, 1993. (b) Gatteschi, D.; Kahn, O.; Miller, J.-S.; Palacio, F. *Magnetic Molecular Materials*; Kluwer Academic: Dordrecht, The Netherlands, 1991. (c) Miller, J.-S. *Adv. Mater.* **2002**, *14*, 1105.

(2) (a) Miller, J.-S.; Epstein, A.-J. *Angew. Chem., Int. Ed. Engl.* **1994**, *33*, 385. (b) Ribas, J.; Escuer, A.; Monfort, M.; Vicente, R.; Cortes, R.; Lezama, L.; Rojo, T. *Coord. Chem. Rev.* **1999**, *195*, 1027. (c) Miller, J.-S.; Epstein, A.-J. *Angew. Chem.* **1994**, *106*, 399. (d) Miller, J.-S., Drilon, M., Eds. *Magnetism: Molecules to Materials*; Wiley-VCH: Weinheim, Germany, 2002−2005, Vols. I−V.

(3) (a) Ribas, J.; Escuer, A.; Monfort, M.; Vicente, R.; Cortés, R.; Lezama, L.; Rojo, T. *Coord. Chem. Rev.* **1999**, *193*, 1027. (b) Wang, X.-Y.; Wang, Z.-M.; Gao, S. *Chem. Commun.* **2008**, *3*, 281. (c) Kurmoo, M. *Chem. Soc. Rev.* **2009**, *38*, 1353.

(4) (a) Yaghi, O. M.; O'Keeffe, M.; Ockwig, N. W.; Chae, H. K.; Eddaoudi, M.; Kim, J. *Nature* **2003**, *423*, 705. (b) James, S. L. *Chem. Soc. Rev.* **2003**, *32*, 276. (c) Glaser, T. *Chem. Commun.* **2011**, *47*, 116. (d) Zhao, D.; Timmons, D. J.; Yuan, D.; Zhou, H.-C. *Acc. Chem. Res.* **2011**, *44*, 123. (e) Sessoli, R.; Powell, A. K. *Coord. Chem. Rev.* **2009**, *253*, 2328.

(5) (a) Winpenny, R. E. P. *J. Chem. Soc., Dalton Trans.* **2002**, 1. (b) Zhang, J.-P.; Huang, X.-C.; Chen, X.-M. *Chem. Soc. Rev.* **2009**, *38*, 2385. (c) Liu, S.; Han, Y.-F.; Jin, G.-X. *Chem. Soc. Rev.* **2007**, *36*, 1543.

(6) (a) Stamatatos, T. C.; Abboud, K. A.; Wernsdorfer, W.; Christou, G. *Angew. Chem., Int. Ed.* **2006**, *45*, 4134. (b) Papaefstathiou, G. S.; Perlepes, S. P.; Escuer, A.; Vicente, R.; Font-Bardía, M.; Solans, X. *Angew. Chem., Int. Ed.* **2001**, *40*, 884. (c) Aromí, G.; Parsons, S.; Wernsdorfer, W.; Brechin, E. K.; McInnes, E. J. L. *Chem. Commun.* **2005**, 5038. (d) Bell, A.; Aromí, G.; Teat, S. J.; Wernsdorfer, W.; Winpenny, R. E. P. *Chem. Commun.* **2005**, 2808. (e) Escuer, A.; Aromí, G. *Eur. J. Inorg. Chem.* **2006**, 4721. (f) Stamatatos, T. C.; Abboud, K. A.; Wernsdorfer, W.; Christou, G. *Angew. Chem., Int. Ed.* **2007**, *46*, 884.

(7) (a) Demeshk, S.; Leibeling, G.; Dechert, S.; Fuchs, S.; Pruschke, T.; Meyer, F. *Chem. Phys. Chem.* **2007**, *8*, 405. (b) Papaefstathiou, G. S.; Escuer, A.; Vicente, R.; Font-Bardía, M.; Solans, X.; Perlepes, S. P. *Chem. Commun.* **2001**, 2414. (c) Zhang, Y.-Z.; Wernsdorfer, W.; Pan, F.; Wang, Z.-M.; Gao, S. *Chem. Commun.* **2006**, 3302. (d) Yang, C. I.; Wernsdorfer, W.; Lee, G. H.; Tsai, H. L. *J. Am. Chem. Soc.* **2007**, *129*, 456. (e) Liu, T.-F.; Fu, D.; Gao, S.; Zhang, Y.-Z.; Sun, H.-L.; Su, G.; Liu, Y.-J. *J. Am. Chem. Soc.* **2003**, *125*, 13976. (f) Escuer, A.; Mautner, F. A.; Goher, M. A. S.; Abu-Youssef, M. A. M.; Vicente, R. *Chem. Commun.* **2005**, 605. (g) Mukherjee, S.; Mukherjee, P. S. *Inorg. Chem.* **2010**, *49*, 10658.

(8) (a) Ju, Z.-F.; Yao, Q.-X.; Wu, W.; Zhang, J. *Dalton Trans.* **2008**, 355. (b) Bitschnau, B.; Egger, A.; Escuer, A.; Mautner, F. A.; Sodin, B.; Vicente, R. *Inorg. Chem.* **2006**, *45*, 868. (c) Escuer, A.; Vicente, R.; Goher, M. A. S.; Mautner, F. A. *J. Chem. Soc., Dalton Trans.* **1997**, 4431. (d) Gao, E.-Q.; Yue, Y.-F.; Bai, S.-Q.; He, Z.; Zhang, S.-W.; Yan, C. H. *Chem. Mater.* **2004**, *16*, 1590. (e) Lazari, G.; Stamatatos, T. C.; Raptopoulou, C. P.; Psycharis, V.; Pissas, M.; Perlepes, S. P.; Boudalis, A. K. *Dalton Trans.* **2009**, 3215. (f) Mondal, K. C.; Mukherjee, P. S. *Inorg. Chem.* **2008**, *47*, 4215.

(9) (a) Sasmal, S.; Hazra, S.; Kundu, P.; Majumder, S.; Aliaga-Alcalde, N.; Ruiz, E.; Mohanta, S. *Inorg. Chem.* **2010**, *49*, 9517.

(b) Sengupta, O.; Mukherjee, P. S. *Inorg. Chem.* **2010**, *49*, 8583. (c) Boonmak, J.; Nakano, M.; Youngme, S. *Dalton Trans.* **2011**, *40*, 1254. (d) Hu, B.-W.; Zhao, J.-P.; Yang, Q.; Zhang, X.-F.; Evangelisti, M.; Sañudo, E. C.; Bu, X.-H. *Dalton Trans.* **2010**, *39*, 11210. (e) Yoon, J. H.; Lee, J. W.; Ryu, D. W.; Yoon, S. W.; Suh, B. J.; Kim, H. C.; Hong, C. S. *Chem.—Eur. J.* **2011**, *17*, 3028. (f) Mukherjee, S.; Gole, B.; Song, Y.; Mukherjee, P. S. *Inorg. Chem.* **2011**, *50*, 3621.

(10) (a) Rodríguez-Fortea, A.; Alemany, P.; Alvarez, S.; Ruiz, E. *Chem.—Eur. J.* **2001**, *7*, 627. (b) Delgado, F. S.; Hernández-Molina, M.; Sanchiz, J.; Ruiz-Pérez, C.; Rodríguez-Martín, Y.; López, T.; Lloret, F.; Julve, M. *CrystEngComm* **2004**, *6*, 106. (c) Mukherjee, P. S.; Konar, S.; Zangrando, E.; Mallah, T.; Ribas, J.; Chaudhuri, N. R. *Inorg. Chem.* **2003**, *42*, 2695. (d) Rao, C. N. R.; Natarajan, S.; Vaidhyanathan, R. *Angew. Chem., Int. Ed.* **2004**, *43*, 1466. (e) Zheng, Y.-Z.; Tong, M.-L.; Zhang, W.-X.; Chen, X.-M. *Angew. Chem., Int. Ed.* **2006**, *45*, 6310.

(11) (a) Zheng, Y.-Z.; Zhang, Y.-B.; Tong, M.-L.; Xue, W.; Chen, X.-M. *Dalton Trans.* **2009**, 1396. (b) Arora, H.; Lloret, F.; Mukherjee, R. *Dalton Trans.* **2009**, 9759. (c) Nytko, E. A.; Helton, J. S.; Müller, P.; Nocera, D. G. *J. Am. Chem. Soc.* **2008**, *130*, 2922. (d) Fabelo, O.; Pasán, J.; Delgado, L. C.; Delgado, F. S.; Lloret, F.; Julve, M.; Pérez, C. R. *Inorg. Chem.* **2008**, *47*, 8053. (e) Caskey, S. R.; Wong-Foy, A. G.; Matzger, A. J. *J. Am. Chem. Soc.* **2008**, *130*, 10870. (f) Coronado, E.; Galán-Mascarós, J. R.; Gómez-García, G. J.; Murcia-Martínez, A. *Chem.—Eur. J.* **2006**, *12*, 3484.

(12) (a) Qin, C.; Wang, X.-L.; Li, Y.-G.; Wang, E.-B.; Su, Z.-M.; Xu, L.; Clérac, R. *Dalton Trans.* **2005**, 2609. (b) Wang, S.-N.; Bai, J.-F.; Xing, H.; Li, Y.-Z.; Song, Y.; Pan, Y.; Scheer, M.; You, X.-Z. *Cryst. Growth Des.* **2007**, *7*, 747. (c) Duan, L.-M.; Xie, F.-T.; Chen, X.-Y.; Chen, Y.; Lu, Y.-K.; Cheng, P.; Xu, J.-Q. *Cryst. Growth Des.* **2006**, *6*, 1101. (d) Coronado, E.; Galán-Mascarós, J. R.; Gómez-García, C. J.; Murcia-Martínez, A. *Chem.—Eur. J.* **2006**, *12*, 3484.

(13) (a) Du, M.; Bu, X.-H.; Guo, Y.-M.; Zhang, L.; Liao, D.-Z.; Ribas, J. *Chem. Commun.* **2002**, 1478. (b) Whitfield, T.; Zheng, L.-M.; Wang, X.; Jacobson, A. J. *Solid State Sci.* **2001**, *3*, 829. (c) Sun, C.-Y.; Zheng, X.-J.; Gao, S.; Li, L.-C.; Jin, L.-P. *Eur. J. Inorg. Chem.* **2005**, 4150. (d) Mahata, P.; Madras, G.; Natarajan, S. *J. Phys. Chem. B* **2006**, *110*, 13759. (e) Tian, H.; Jia, Q.-X.; Gao, E.-Q.; Wang, Q.-L. *Chem. Commun.* **2010**, 5349.

(14) (a) Liu, T.; Zhang, Y.-J.; Wang, Z.-M.; Gao, S. *Inorg. Chem.* **2006**, *45*, 2782. (b) Milios, C. J.; Prescimone, A.; Sanchez-Benitez, J.; Parsons, S.; Murrie, M.; Brechin, E. K. *Inorg. Chem.* **2006**, *45*, 7053. (c) Wang, X.-T.; Wang, X.-H.; Wang, Z.-M.; Gao, S. *Inorg. Chem.* **2009**, *48*, 1301. (d) Thompson, L. K.; Tandon, S. S.; Lloret, F.; Cano, J.; Julve, M. *Inorg. Chem.* **1997**, *36*, 3301. (e) Li, L.-C.; Liao, D.-Z.; Jiang, Z.-H.; Yan, S.-P. *Polyhedron* **2001**, *20*, 681. (f) Meyer, F.; Demeshko, S.; Leibeling, G.; Kersting, B.; Kaifer, E.; Pritzkow, H. *Chem.—Eur. J.* **2005**, *11*, 1518.

(15) (a) Youngme, S.; Chotkhun, T.; Leelasubcharoen, S.; Chaichit, N.; van Albada, G. A.; Viciano-Chumillas, M.; Reedijk, J. *Inorg. Chem. Commun.* **2007**, *10*, 109. (b) Demeshko, S.; Leibeling, G.; Maringgele, W.; Meyer, F.; Mennerich, C.; Klauss, H. H.; Pritzkow, H. *Inorg. Chem.* **2005**, *44*, 519. (c) Mondal, K. C.; Sengupta, O.; Nethaji, M.; Mukherjee, P. S. *Dalton Trans.* **2008**, 767. (d) Chen, Z.-L.; Jiang, C.-F.; Yan, W.-H.; Liang, F.-P.; Batten, S. R. *Inorg. Chem.* **2009**, *48*, 4674. (e) Zhao, J.-P.; Hu, B.-W.; Sanudo, E. C.; Yang, Q.; Zeng, Y.-F.; Bu, X.-H. *Inorg. Chem.* **2009**, *48*, 2482. (f) Tong, M.-L.; Hong, C.-G.; Zheng, L.-L.; Peng, M.-X.; Gaita-Ariño, A.; Modesto, J.; Clemente, J. *Eur. J. Inorg. Chem.* **2007**, 3710.

(16) (a) Escuer, A.; Vicente, R.; Mautner, F. A.; Goher, M. A. S. *Inorg. Chem.* **1997**, *36*, 1233. (b) Han, Y.-F.; Wang, T.-W.; Song, Y.; Shen, Z.; You, X.-Z. *Inorg. Chem. Commun.* **2008**, *11*, 207. (c) Zhao, J.-P.; Hu, B.-W.; Sanudo, E. C.; Yang, Q.; Zeng, Y.-F.; Bu, X.-H. *Inorg. Chem.* **2009**, *48*, 2482.

(17) (a) Ma, Y.; Zhang, J.-Y.; Cheng, A.-L.; Sun, Q.; Gao, E.-Q.; Liu, C.-M. *Inorg. Chem.* **2009**, *48*, 6142. (b) Ma, Y.; Wang, K.; Gao, E.-Q.; Song, Y. *Dalton Trans.* **2010**, *39*, 7714. (c) Wang, Y.-Q.; Zhang, J.-Y.; Jia, Q.-X.; Gao, E.-Q.; Liu, C.-M. *Inorg. Chem.* **2009**, *48*, 789. (d) Sun, W.-W.; Tian, C.-Y.; Jing, X.-H.; Wang, Y.-Q.; Gao, E.-Q. *Chem. Commun.* **2009**, 4741. (e) Ma, Y.; Wen, Y.-Q.; Zhang, J.-Y.; Gao, E.-Q.; Liu, C.-M. *Dalton Trans.* **2010**, *39*, 1846. (f) Jia, Q.-X.; Tian, H.; Zhang, J.-Y.; Gao, E.-Q. *Chem.—Eur. J.* **2011**, *17*, 1040.

(18) (a) Wang, Y.-Q.; Jia, Q.-X.; Wang, K.; Cheng, A.-L.; Gao, E.-Q. *Inorg. Chem.* **2010**, *49*, 1551. (b) Tian, C.-Y.; Sun, W.-W.; Jia, Q.-X.; Tian, H.; Gao, E.-Q. *Dalton Trans.* **2009**, 6109. (c) Zhang, X.-M.; Wang, Y.-Q.; Wang, K.; Gao, E.-Q.; Liu, C.-M. *Chem. Commun.* **2011**, 1815. (d) Ma, Y.; Li, X.-B.; Yi, X.-C.; Jia, Q.-X.; Gao, E.-Q.; Liu, C.-M. *Inorg. Chem.* **2010**, *49*, 8092.

(19) (a) Zeng, Y.-F.; Hu, X.; Liu, F.-C.; Bu, X.-H. *Chem. Soc. Rev.* **2009**, *38*, 496. (b) Liu, F.-C.; Zeng, Y.-F.; Zhao, J.-P.; Hu, B.-W.; Sanudo, E.-C.; Ribas, J.; Bu, X.-H. *Inorg. Chem.* **2007**, *46*, 7698. (c) Liu, F.-C.; Zeng, Y.-F.; Li, J.-R.; Bu, X.-H.; Zhang, H.-J.; Ribas, J. *Inorg. Chem.* **2005**, *44*, 7298. (d) Zeng, Y.-F.; Liu, F.-C.; Zhao, J.-P.; Cai, S.; Bu, X.-H.; Ribas, J. *Chem. Commun.* **2006**, 2227. (e) Hu, B.-W.; Zhao, J.-P.; Sanudo, E.-C.; Liu, F.-C.; Zeng, Y.-F.; Bu, X.-H. *Dalton Trans.* **2008**, 5556. (f) Chen, H.-J.; Mao, Z.-W.; Gao, S.; Chen, X.-M. *Chem. Commun.* **2001**, 2320.

(20) (a) Zhao, J.-P.; Hu, B.-W.; Zhang, X.-F.; Yang, Q.; Elfallah, M. S.; Ribas, J.; Bu, X.-H. *Inorg. Chem.* **2010**, *49*, 11325. (b) Liu, F.-C.; Zhao, J.-P.; Hu, B.-W.; Zeng, Y.-F.; Ribasc, J.; Bu, X.-H. *Dalton Trans.* **2010**, *39*, 1185.

(21) Sheldrick, G. M. *Program for Empirical Absorption Correction of Area Detector Data*; University of Göttingen: Göttingen, Germany, 1996.

(22) Sheldrick, G. M. *SHELXTL*, version 5.1; Bruker Analytical X-ray Instruments Inc.: Madison, WI, 1998.

(23) Spek, A. L. *J. Appl. Crystallogr.* **2003**, *36*, 7.

(24) Addison, W.; Rao, T. N.; Reedijk, J.; van Rijn, J.; Verschoor, G. C. *J. Chem. Soc., Dalton Trans.* **1984**, 1349.

(25) (a) Brown, I. D.; Altermatt, D. *Acta Crystallogr.* **1985**, *B41*, 244. (b) Liu, W.-T.; Thorp, H. H. *Inorg. Chem.* **1993**, *32*, 4102.

(26) Baker, G. A.; Rushbrooke, G. S.; Gilbert, H. E. *Phys. Rev. A* **1964**, *135*, 1272.

(27) O'Connor, C. J. *Prog. Inorg. Chem.* **1982**, *29*, 203.

(28) Carlin, R. L. *Magnetochemistry*; Springer: Berlin, 1986.

(29) (a) Menelaou, M.; Raptopoulou, C. P.; Terzis, A.; Tangoulis, V.; Salifoglou, A. *Eur. J. Inorg. Chem.* **2006**, 1957. (b) de Jongh, L. J.; Miedema, A. R. *Adv. Phys.* **1974**, *23*, 220.

(30) Bleaney, B.; Bowers, K. D. *Proc. R. Soc. London, Ser. A* **1952**, *214*, 451.

(31) Tandon, S. S.; Thompson, L. K.; Manuel, M. E.; Bridson, J. N. *Inorg. Chem.* **1994**, *33*, 5555.

(32) Ruiz, E.; Cano, J.; Alvarez, S.; Alemany, P. *J. Am. Chem. Soc.* **1998**, *120*, 11122.

(33) (a) Nishida, Y.; Takeuchi, M.; Takahashi, K.; Kida, S. *Chem. Lett.* **1985**, 631. (b) Nishida, Y.; Takeuchi, M.; Takahashi, K.; Kida, S. *Chem. Lett.* **1983**, 1815. (c) McKee, V.; Zvagulis, M.; Reed, C. A. *Inorg. Chem.* **1985**, *24*, 2914.

(34) (a) Biswas, C.; Drew, M. G. B.; Ruiz, E.; Estrader, M.; Diaz, C.; Ghosh, A. *Dalton Trans.* **2010**, *39*, 7474. (b) Youngme, S.; Chotkhun, T.; Leelasubcharoen, S.; Chaichit, N.; van Albada, G. A.; Viciano-Chumillas, M.; Reedijk, J. *Inorg. Chem. Commun.* **2009**, *10*, 109. (c) Boillot, M.-L.; Kahn, O.; O'Connor, C. J.; Gouteron, J.; Jeannin, S.; Jeanninb, Y. *J. Chem. Soc., Chem. Commun.* **1985**, 178. (d) You, Z.-L.; Jiao, Q.-Z.; Niu, S.-Y.; Chi, J.-Y. *Z. Anorg. Allg. Chem.* **2006**, *632*, 2481.

(35) (a) Zeng, Y.-F.; Zhao, J.-P.; Hu, B.-W.; Hu, X.; Liu, F.-C.; Ribas, J.; Ribas-Ariño, J.; Bu, X.-H. *Chem.—Eur. J.* **2007**, *13*, 9924. (b) Tangoulis, V.; Panagoulis, D.; Raptopoulou, C. P.; Dendrinou-Samara, C. *Dalton Trans.* **2008**, 1752. (c) Thompson, L. K.; Tandon, S. S.; Lloret, F.; Cano, J.; Julve, M. *Inorg. Chem.* **1997**, *36*, 3301. (d) Escuer, A.; Vicente, R.; Mautner, F. A.; Goher, M. A. S. *Inorg. Chem.* **1997**, *36*, 1233. (e) He, Z.; Wang, Z.-M.; Gao, S.; Yan, C.-H. *Inorg. Chem.* **2006**, *45*, 6694. (f) Han, Y.-F.; Wang, T.-W.; Song, Y.; Shen, Z.; You, X.-Z. *Inorg. Chem. Commun.* **2008**, *11*, 207. (g) Kostakis, G. E.; Mondal, K. C.; Abbas, G.; Lan, Y.; Novitchi, G.; Buth, G.; Ansonb, C. E.; Powell, A. K. *CrystEngComm* **2009**, *11*, 2084.

(36) Sun, W.-W.; Cheng, A.-L.; Jia, Q.-X.; Gao, E.-Q. *Inorg. Chem.* **2007**, *46*, 5471.

(37) (a) Georges, R.; Borrás-Almenar, J. J.; Coronado, E.; Curély, J.; Drillon, M. *Magnetism: Molecules to Materials I: Models and Experiments*; Wiley: New York, 2003; Vol. I, p 22. (b) Fisher, M. E. *Am. J. Phys.* **1964**, *32*, 343.

(38) (a) Weng, C. H. Ph.D. Dissertation, Carnegie-Mellon University, Pittsburgh, PA, 1968. (b) Hiller, W.; Strahle, J.; Datz, A.; Hanack, M.; Hatfield, W. E.; ter Haar, L. W.; Gutlich, P. *J. Am. Chem. Soc.* **1984**, *106*, 329.

(39) Escuer, A.; Vicente, R.; Goher, M. A. S.; Mautner, F. A. *Inorg. Chem.* **1996**, *35*, 6386.

(40) Ma, Y.; Bandeira, N. A. G.; Robert, V.; Gao, E.-Q. *Chem.—Eur. J.* **2011**, *17*, 1988.

(41) (a) Ghosh, A. K.; Ghoshal, D.; Zangrando, E.; Ribas, J.; Chaudhuri, N. R. *Inorg. Chem.* **2005**, 1786. (b) Sra, A. K.; Sutter, J.-P.; Guionneau, P.; Chasseau, D.; Yakhmi, J. V.; Kahn, O. *Inorg. Chim. Acta* **2000**, *300*−*302*, 778. (c) Abu-Youssef, M. A. M.; Escuer, A.; Langer, V. *Eur. J. Inorg. Chem.* **2005**, 4659. (d) Abu-Youssef, M. A. M.; Escuer, A.; Langer, V. *Eur. J. Inorg. Chem.* **2006**, 3177. (e) Wen, H.-R.; Wang, C.-F.; Song, Y.; Zuo, J.-L.; You, X.-Z. *Inorg. Chem.* **2005**, *44*, 9039. (f) Song, X.-Y.; Xu, Y.-h.; Li, L.-C.; Jiang, Z.-H.; Liao, D.-Z. *Inorg. Chem. Commun.* **2006**, *9*, 1212. (g) Gao, E.-Q.; Cheng, A.-L.; Xu, Y.-X.; He, M.-Y.; Yan, C.-H. *Inorg. Chem.* **2005**, *44*, 8822.